

# Memory Effects are Relevant for Chaotic Advection of Inertial Particles

Anton Daitche

*Institute for Theoretical Physics, Münster University, Wilhelm-Klemm-Straße 9, D-48149 Münster, Germany*

Tamás Tél

*Institute for Theoretical Physics, Eötvös University, Pázmány Péter sétány 1/A, H-1117 Budapest, Hungary*  
(Received 27 June 2011; published 5 December 2011)

A systematic investigation of the effect of the history force on particle advection is carried out in a paradigmatic model flow of chaotic advection, the von Kármán flow. All investigated properties turn out to heavily depend on the presence of memory when compared to previous studies neglecting this force. We find a weaker tendency for accumulation and for caustics formation. The Lyapunov exponent of transients becomes larger, the escape rates are strongly altered. Attractors are found to be suppressed by the history force, and periodic ones have a very slow,  $t^{-1/2}$ -type convergence towards the asymptotic form.

DOI: 10.1103/PhysRevLett.107.244501

PACS numbers: 47.52.+j, 05.45.-a, 47.55.Kf

Chaotic advection of finite-size particles (often called inertial particles) plays an important role in many environment-related phenomena ranging from meteorology to oceanography (for a recent review, see [1]). The advection of such particles is known to be important in the understanding of cloud microphysics [2,3]. Timely applications are pollutant-transport forecasting for homeland defense [4] and the location of a toxin or biological pathogen spill (e.g., anthrax) from outbreaks in a street canyon [5]. Other recent results indicate that inertial particles might play a role in hurricane dynamics [6] and in the feeding dynamics of certain marine animals [7]. Particle-based modeling of aggregation and fragmentation has been recently examined in [8].

The basic equations of motion for small spherical particles in a viscous fluid are given by the Maxey-Riley (MR) equation [9,10]. Their precise form contains an integral, also called the history (or Basset) force, which describes the diffusion of vorticity around the particle during its full time history. This term renders the advection equation to be an integro-differential equation whose solution is much more demanding than that of an ordinary differential equation. Because of this difficulty, the integral term is neglected in nearly all the applications mentioned above. A qualitative argument for this is that both the Stokes drag and the history force describe dissipative effects, and keeping the simpler one, the Stokes drag, might be sufficient to describe the essence. The MR equation without the integral term clearly shows that the Hamiltonian passive advection problem is converted, due to the drag, into a dissipative problem which can have attractors, and correspondingly, inertial particles can have the tendency to accumulate in certain regions of the flow [11] (a phenomenon termed preferential concentration). Experimental and analytic efforts [12,13] indicate, however, that the history force might have significant effects for non-neutrally buoyant particles in simple flows, and so do perturbative treatments of

weakly inertial particles in chaotic flows [14,15], as well as investigations in turbulent flows (see, e.g., [16]).

Our aim here is to consider the nonperturbative description of memory effects on inertial particles in chaotic flows. The emphasis will not be on the deviation between trajectories with and without memory (since they deviate anyhow due to the sensitivity to initial conditions), rather it will be on the deviation in *statistical* properties. We shall point out that properties like, e.g., the escape rate of particle ensembles basically differ due to the history force both for bubbles and aerosols (particles lighter and heavier than the fluid). One important effect of memory is that attractors can disappear, and that the tendency for caustics formation is weaker than with Stokes drag only. The average Lyapunov exponent of the transients is typically larger than without memory. We find in general that memory effects may strongly alter inertial effects, so that even qualitative changes can occur.

The dimensionless MR equation of a small, rigid, spherical particle of radius  $a$  and density  $\rho_p$  in a fluid of kinematic viscosity  $\nu$  and density  $\rho_f$  in velocity field  $\mathbf{u}(\mathbf{r}, t)$  reads as [9,10]

$$\frac{d\mathbf{v}}{dt} = \frac{3}{2} R \frac{D\mathbf{u}}{Dt} - A(\mathbf{v} - \mathbf{u}) - \sqrt{\frac{9AR}{2\pi}} \int_{t_0}^t \frac{\frac{d(\mathbf{v}-\mathbf{u})}{d\tau}}{\sqrt{t-\tau}} d\tau, \quad (1)$$

where  $\mathbf{v} \equiv d\mathbf{r}/dt$  is the particle velocity,  $d\mathbf{u}/dt$  and  $D\mathbf{u}/Dt$  denote the full derivative along the trajectory of the particle and of the corresponding fluid element, respectively. In this form gravity is not included, and the initial particle velocity should match that of the fluid:  $\mathbf{v}_0 = \mathbf{u}_0$ . One important parameter is the density ratio  $R = 2\rho_f/(\rho_f + 2\rho_p)$ . The other one is the inertial parameter  $A = R/St$ , a dimensionless relaxation rate to the fluid in which the Stokes number  $St = (2a^2U)/(9L\nu)$  denotes the ratio of the viscous relaxation time and the characteristic

time of the flow. In smooth flows, which we assume here, this is estimated as the ratio  $L/U$  of the characteristic length and velocity scales. Conditions for the validity of (1) are that the particle Reynolds number  $\text{Re}_p = |\mathbf{v} - \mathbf{u}|a/\nu$  remains small during the entire dynamics and that the Stokes number and  $a/L$  are small [9]. The last condition assures that the so-called Faxen corrections are negligible. The terms on the right-hand side of (1) are the force exerted by the fluid on a fluid element at the location of the particle including the added mass effect, the Stokes drag, and the history force [9]. Being interested in the effect of the latter, effects due to the lift force or corrections due to finite particle Reynolds number are not taken into account.

Equation (1) is a second order integro-differential equation for the trajectory  $\mathbf{r}(t)$  of an inertial particle. To any initial condition  $(\mathbf{r}_0, \mathbf{v}_0)$  at time  $t_0$  there is a unique trajectory, but the transition between infinitesimally close neighboring time instants  $t$  and  $t + dt$  does not only depend on the state  $(\mathbf{r}(t), \mathbf{v}(t))$ , but also on all the previous instants. Therefore a stroboscopic map taken at integer multiples of some time unit turns out to be *nonautonomous*. This is a nonstandard problem, in which novel features can show up also from a dynamical systems point of view.

There are several difficulties arising when one tries to treat the history force numerically. On the one hand, the integral term contains  $d\mathbf{v}/dt$ , which makes the MR equation implicit. On the other hand, an integral over the whole history has to be evaluated for every time step of the integration scheme, so that the computational costs grow with the square of the number of time steps. For large particle ensembles they become so high that the computational time can be kept feasible only with parallel computation. Here we sketch the solution of one problem only, namely, the treatment of the singular kernel appearing in the integral term. The idea we present is crucial in the development of higher order numerical integration schemes. The singularity appearing at  $\tau = t$  is integrable but cannot be treated well by ordinary Newton-Cotes schemes, as these always produce an error of order  $h^{1/2}$  for time step  $h$ . We need to treat the singularity analytically. To this end we slice up the integral into time intervals  $[\tau_i, \tau_{i+1}]$  of length  $h$  and approximate only the function  $f(\tau) = d(\mathbf{v} - \mathbf{u})/d\tau$  by a polynomial, but not the kernel. The remaining integrals can be solved analytically, leading to a quadrature which does not contain any singular expressions. When using a first order polynomial, i.e.,  $f(\tau) = f(\tau_i) + (\tau - \tau_i)[f(\tau_{i+1}) - f(\tau_i)]/h$ , we obtain a first order scheme

$$\begin{aligned} \int_{t_0}^t \frac{f(\tau)}{\sqrt{t - \tau}} d\tau &= 2f(t_0)\sqrt{t - t_0} + \mathcal{O}(h^2)\sqrt{t - t_0} \\ &+ \frac{4}{3} \sum_{i=0}^{N-1} \frac{f(\tau_{i+1}) - f(\tau_i)}{h} \\ &\times [(t - \tau_i)^{3/2} - (t - \tau_{i+1})^{3/2}]. \quad (2) \end{aligned}$$

This scheme is equivalent to the one in [17] even though this is not easily seen. We have also developed schemes of second and third order (with errors proportional to  $h^3$  and  $h^4$ ), which we omit here because of their complexity. The third order quadrature scheme combined with a third order Adams-Basforth-Moulton predictor-corrector scheme has been used to obtain the results presented here. The order of the whole integration scheme has been verified using the analytical solution to the problem of a particle in a single vortex [13].

We consider a spatially smooth, two-dimensional time-periodic flow for the velocity field  $\mathbf{u}$ . As a paradigmatic example, we consider the von Kármán flow in the wake of a cylinder as described in [18]. This analytical flow was shown to faithfully represent the Navier-Stokes dynamics at  $\text{Re} \approx 250$  and has been used in recent studies of inertial particles as well [19,20]. The radius of the cylinder is chosen to be the length unit  $L$ , and velocity is measured in units of  $U = L/T$  where  $T$  is the period of vortex shedding. The stream function of the model is taken from the literature [21]. An important flow parameter is the dimensionless strength  $w$  of the vortices (for comparison with [21] we first take  $w = 192/\pi$  and later use  $w = 24$ ).

First, we consider trajectories starting with the same initial condition and compare different approximations (Fig. 1). One immediately observes that the trajectory with memory is in between the other two. The force acting on the particle can be decomposed into the three contributions on the right-hand side of (1). The terms, called the pressure force, the Stokes drag, and the history force, are marked by different arrows at subsequent time instants in Fig. 1. As the legend indicates, only one quarter of the pressure force is given, for better visibility. We thus clearly see that the pressure force always dominates the other two, but the history force is often larger than the drag. A comparison of the full trajectory with that obtained without memory shows that the direction of separation of these trajectories coincides with the direction of the history

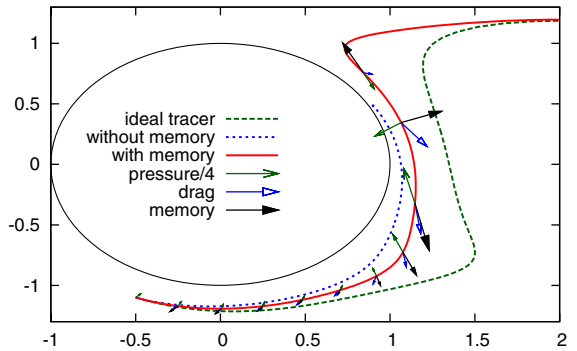


FIG. 1 (color online). Trajectories of a bubble (i.e.,  $R > 2/3$ ) with and without memory ( $R = 1.7$ ,  $A = 40$ ,  $w = 192/\pi$ ) and an ideal tracer, all starting at  $t_0 = 0$ ,  $\mathbf{r}_0 = (-0.5, -1.1)$ . The forces acting on a particle with memory are shown as arrows.

force. We have found similar tendencies for aerosols, e.g., for  $R = 0.5$ .

Next, we turn to the dynamics of ensembles of non-interacting particles. A large number  $N_0 \approx 1.8 \times 10^6$  of particles is distributed uniformly around the cylinder. All particles are followed up to a certain time when we plot their position. The results are shown in Fig. 2. A filamentary pattern can be seen with and without memory. This is in itself an indication for the chaoticity of the advection dynamics in both cases. Since the problem is dissipative, attractors might also be present, but the emptying process is always of transient type when the underlying chaotic set is a chaotic saddle [22,23]. The two distributions shown trace out the unstable manifold of the saddle with and without memory. They differ both in large and small scale structures. A characteristic feature of the case without memory is the appearance of caustics [2,24], i.e., the intersection of different branches in the configuration space. This is due to the fact that what we see is a projection of the full pattern in the four-dimensional  $(x, y, v_x, v_y)$  phase space to a plane. Caustics appear with a *much lower* probability in the presence of memory, indicating that the dependence on the velocity coordinates is weaker in this case. A similar result has also been found for other  $R$  values, e.g., for  $R = 0.3, 0.5, 1.0, 1.2, 1.5$ . A quantity closely related to caustics is the collision rate. For the parameters given in Fig. 2 and a collision distance equal to the particle size, we have found the time-averaged collision rate [25] with memory to be reduced to 1/4 of that without memory.

The decay dynamics is best followed by monitoring the total number of particles that have not yet escaped a given region. We distribute  $N_0 \approx 1.5 \times 10^6$  particles uniformly in the domain  $[0.6, 4] \times [-2, 2]$  outside the cylinder. A quantitative measure characterizing the emptying of the wake is the escape rate  $\kappa$  that can be obtained from the number  $N(t)$  of nonescaped particles at time  $t$ . After some time, it decays exponentially, i.e.,  $N(t) \sim \exp(-\kappa t)$ . A particle is considered to have escaped if it crosses the line  $x = 5$  or it enters a circle of radius  $r = 1.014$  around

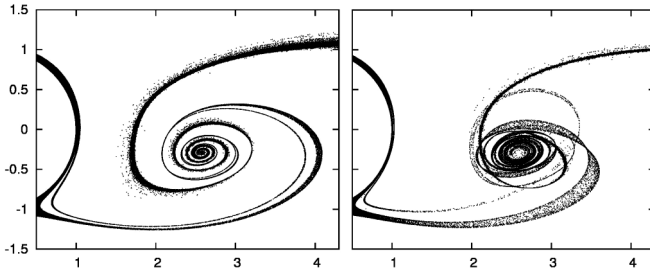


FIG. 2. Distribution of an ensemble of  $N_0 \approx 1.8 \times 10^6$  bubbles ( $R = 1.7$ ,  $A = 40$ ,  $w = 192/\pi$ ) at  $t = 1.1$ , started in the domain  $[-1, 4] \times [-2, 2]$  around the cylinder at  $t_0 = 0.2$ . The left (right) figure shows the case with (without) memory. See Supplemental Material [28] for an animation of the ensemble dynamics.

the cylinder. Using a circle larger in radius than the cylinder is motivated by excluding very slow (nonhyperbolic) decay characterizing the boundary layer, as done in [4,21].

The escape rate depends on both dimensionless parameters of the advection problem,  $R$  and  $A$ . The  $A$  dependence for fixed density ratios is shown in Fig. 3. It is clear that the escape rate of bubbles without memory is much below the escape rate of ideal tracers. Moreover, in a broad interval of  $A$  values attractors appear where the escape rate formally takes on the value 0 (see [21] for details). For the escape rate of bubbles with memory we find a considerable *increase*,  $\kappa$  still remains below the ideal value, but never goes down to zero. The latter implies that attractors are *much less typical* for the full problem than for the one without memory. Figure 3 also shows the escape rate for aerosols, for which attractors are not found in any case. The main effect of memory is the *reduction* of escape rate. The new escape rate is, however, always larger than for ideal tracers. Thus aerosols leave the wake on average faster than in the ideal case, but slower than without memory. Memory effects have been found to be essential for all the  $R$  values mentioned earlier. The increased (decreased) escape rate for bubbles (aerosols) with memory can be explained by the fact that the history force generates a *countereffect* to the centrifugal force. For bubbles, it points away from the center of the tangent circle drawn to the trajectory, as Fig. 1 indicates (see also [13]).

As a quantitative measure of chaos, we determine the average Lyapunov exponent. Since in the cases investigated no chaotic attractors have been found, we deal with the Lyapunov exponent of transient chaos. To this end, we consider particles with lifetime longer than 20 time units. The initial position of such particles should lie close to the stable manifold of a chaotic saddle. To any particle with lifetime longer than 20 in the domain  $[-1, 4] \times [-2, 2]$  we associate a test particle of small initial distance. The logarithmic distance between the original and test particles is followed up to escape and averaged over all initial conditions. We have found that the inclusion of the history force leads to an increase of the average Lyapunov

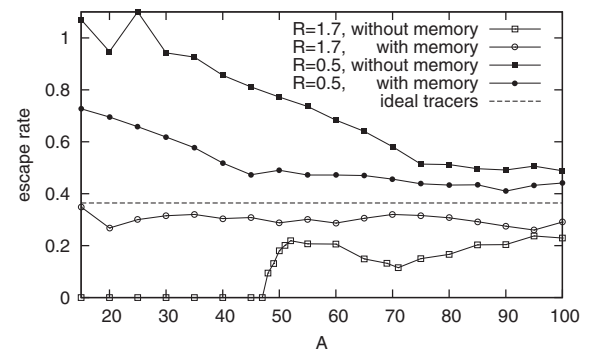


FIG. 3. Escape rate for bubbles ( $R = 1.7$ ) and aerosols ( $R = 0.5$ ) as a function of the inertial parameter  $A$  ( $w = 192/\pi$ ).

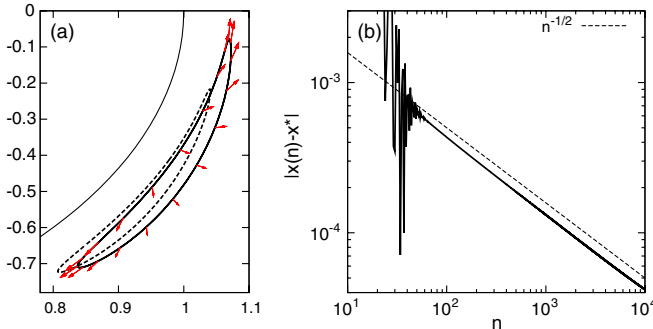


FIG. 4 (color online). (a) Attractors with and without memory (solid line and dashed line, respectively) traced out by approaching trajectories after  $10^4$  time units (the parameters are  $R = 1.33$ ,  $A = 30$ ,  $w = 24$ ). The arrows show the history force. (b) Distance between an approaching trajectory with memory and the corresponding attractor at integer times.

exponent for both bubbles and aerosols, but the Lyapunov exponent always stays below the one for ideal tracers ( $\lambda = 0.92$ ). To give some examples: For parameters  $R = 1.7$ ,  $A = 80$  ( $R = 0.5$ ,  $A = 80$ ), we find  $\bar{\lambda} = 0.91$  ( $\bar{\lambda} = 0.79$ ) with memory and  $\bar{\lambda} = 0.84$  ( $\bar{\lambda} = 0.70$ ) without. As a function of  $A$  we have found the average Lyapunov exponent to increase monotonically in the range  $A \in [20, 100]$  in both cases.

Let us now turn to vortex strength values where attractors are still present with memory, as is the case for  $w = 24$ . When comparing the attractor with and without memory, we see that both attracting objects appear to be periodic orbits (with the period of vortex shedding), and are of similar form, as Fig. 4(a) shows. We investigate the convergence of the trajectory through the quantity  $|x(n) - x^*|$ , where  $x(n)$  and  $x^*$  are the  $x$  coordinates of an approaching trajectory and the attractor at multiples of the period. Figure 4(b) shows a very slow algebraic convergence with memory in contrast to an exponential convergence without memory (not shown). The power law convergence  $t^{-1/2}$  is obviously related to the power law behavior of the kernel in (1). The fact that a precisely periodic attractor sets in can be explained by the observation that after a very long time the memory of the approach to the attractor decays away, and the dynamics remembers only what has been in the close vicinity of the attractor and a convergence becomes thus possible. Note that the history force on the attractor does not vanish.

Among the aspects we investigated but cannot present in detail, we mention that the periodic attractors found have considerably *smaller* basins than their memoryless counterparts. The chaotic saddles and their manifolds differ essentially. Surprisingly, in a narrow region around  $w = 31.2$ ,  $R = 1.47$ ,  $A = 40$  even a chaotic attractor has been found where only a periodic attractor exists without memory, a phenomenon deserving further investigation. Neutrally buoyant particles ( $R \approx 2/3$ ) are known to form

a distinct case [19,26,27]; the study of the memory effects in such cases is beyond the scope of this Letter.

In summary, memory effects have an essential influence on inertial particles. They lead to a suppression of chaotic attractors and, more generally, to a weaker tendency for preferential concentration and caustics formation. The dynamical instability remains strong. Our findings suggest that memory effects cannot, in general, be neglected. In certain cases they “push” the dynamics towards the ideal case, but let it nevertheless be different in many interesting aspects.

It is worth noting that one often argues that the history force becomes negligible for heavy particles, i.e., in the limit  $R \rightarrow 0$ . Equation (1) seems to support this view, provided  $A$  remains constant. Note, however, that  $A$  is proportional to  $R$ , and thus, for fixed St, the ratio of the integral and the Stokes term is *independent* of the density. We can thus say that statements from the literature on inertial particles, that have been considered well grounded, should be reconsidered from the point of view of memory effects. These include the transport of pollutant and toxic materials, and also of heavy particles, which play an essential role in cloud microphysics.

Useful discussions with J.-R. Angilella, I. Benczik, U. Feudel, and M. Wilczek are acknowledged. The project is supported by Grants No. TAMOP 4.2.1./B-09/1/KMR-2010-0003 and No. OTKA NK72037. The support of the Alexander von Humboldt Foundation is also acknowledged.

- 
- [1] F. Toschi and E. Bodenschatz, *Annu. Rev. Fluid Mech.* **41**, 375 (2009).
  - [2] G. Falkovich, A. Fouxon, and M. Stepanov, *Nature (London)* **419**, 151 (2002).
  - [3] G. Falkovich and A. Pumir, *J. Atmos. Sci.* **64**, 4497 (2007).
  - [4] I. J. Benczik, Z. Toroczkai, and T. Tél, *Phys. Rev. Lett.* **89**, 164501 (2002).
  - [5] W. Tang, G. Haller, J.-J. Baik, and Y.-H. Ryu, *Phys. Fluids* **21**, 043302 (2009).
  - [6] T. Sapsis and G. Haller, *J. Atmos. Sci.* **66**, 2481 (2009).
  - [7] T. Sapsis, J. Peng, and G. Haller, *Bull. Math. Biol.* **73**, 1841 (2011).
  - [8] J. C. Zahnow, J. Maerz, and U. Feudel, *Physica (Amsterdam)* **240D**, 882 (2011).
  - [9] M. R. Maxey and J. J. Riley, *Phys. Fluids* **26**, 883 (1983).
  - [10] T. R. Auton, J. C. R. Hunt, and M. Prud'Homme, *J. Fluid Mech.* **197**, 241 (1988).
  - [11] J. Bec, L. Biferale, M. Cencini, A. Lanotte, S. Musacchio, and F. Toschi, *Phys. Rev. Lett.* **98**, 084502 (2007).
  - [12] N. Mordant and J. Pinton, *Eur. Phys. J. B* **18**, 343 (2000).
  - [13] F. Candelier, J. R. Angilella, and M. Souhar, *Phys. Fluids* **16**, 1765 (2004).
  - [14] O. A. Druzhinin and L. Ostrovsky, *Physica (Amsterdam)* **76D**, 34 (1994).

- [15] A. N. Yannacopoulos, G. Rowlands, and G. P. King, *Phys. Rev. E* **55**, 4148 (1997).
- [16] V. Armenio and V. Fiorotto, *Phys. Fluids* **13**, 2437 (2001).
- [17] M. van Hinsberg, J. ten Thije Boonkkamp, and H. Clercx, *J. Comput. Phys.* **230**, 1465 (2011).
- [18] C. Jung, T. Tél, and E. Ziemniak, *Chaos* **3**, 555 (1993).
- [19] T. Sapsis and G. Haller, *Phys. Fluids* **20**, 017102 (2008).
- [20] G. Haller and T. Sapsis, *Physica (Amsterdam)* **237D**, 573 (2008).
- [21] I.J. Benczik, Z. Toroczkai, and T. Tél, *Phys. Rev. E* **67**, 036303 (2003).
- [22] E. Ott, *Chaos in Dynamical Systems* (Cambridge University Press, Cambridge, England, 2002), 2nd ed.
- [23] T. Tél and M. Gruiz, *Chaotic Dynamics* (Cambridge University Press, Cambridge, England, 2006).
- [24] M. Wilkinson and B. Mehlig, *Europhys. Lett.* **71**, 186 (2005).
- [25] Let  $C(t)$  be the set of particle pairs with distance smaller than the collision distance and  $\Delta t$  a small time interval. The collision rate is the number of particle pairs in the set  $C(t) \setminus C(t - \Delta t)$  divided by  $N(t)^2 \Delta t / 2$ . The time average of the collision rate was performed in the time interval [1,10] for particles started in  $[-1, 4] \times [-2, 2]$  and not yet escaped from the flow.
- [26] A. Babiano, J. H. E. Cartwright, O. Piro, and A. Provenzale, *Phys. Rev. Lett.* **84**, 5764 (2000).
- [27] E. Calzavarini, R. Volk, E. Leveque, J.-F. Pinton, and F. Toschi, [arXiv:1008.2888](https://arxiv.org/abs/1008.2888).
- [28] See Supplemental Material at <http://link.aps.org-supplemental/10.1103/PhysRevLett.107.244501> for an animation of the ensemble dynamics.